Science in China Series F: Information Sciences

New theoretical framework for OFDM/CDMA systems with peak-limited nonlinearities

WANG Jian†, ZHANG Lin, SHAN XiuMing & REN Yong

Department of Electronic Engineering, Tsinghua University, Beijing 100084, China

A new theoretical framework for the evaluation of the in-band nonlinear distortion effects on the performance of OFDM systems is presented. In contrast to previous works that approximate the nonlinear noise as a Gaussian additive random process, the new framework is based on the properties of the large deviations of a stationary Gaussian process and shot noise theories, which can evaluate the performance of the OFDM system with high accuracy, especially at realistic scenarios where the Gaussian approximation of the nonlinear noise is no longer valid. The approach can be used to evaluate many communication systems with peak-limited nonlinearities and high PAPR, such as the downlink performance analysis of large capacity DS-CDMA systems.

OFDM, CDMA, nonlinearities, impulse noise

OFDM is a promising candidate for achieving high data rate transmission in wireless environment and is widely employed in communication systems. Since an OFDM signal is the sum of several statistically independent random subcarriers, its baseband in-phase/quadrature (I/Q) components can be approximately represented as a Gaussian process with Rayleigh envelope distribution and uniform phase distribution invoking the Central Limit Theorem[1]. Simulation results show that the Gaussian approximation is very realistic for most of the practical systems of interest with a sufficiently large number of subcarriers. One of the major drawbacks of a nearly Gaussian OFDM waveform is a greatly variable envelope or high peak-to-average power ratio (PAPR) that makes it particularly sensitive to nonlinear distortions, such as analog-to-digital (A/D) converters, IFFT/FFT processors with finite word length, RF high power amplifiers (HPA), etc., which will cause both in-band and out-of-band distortion.

It has been shown that the out-of-band distortion can be removed using a simple filter without adding any distortion to the signal[2]. Recently, several different methods have been derived for analysis of in-band distortion of OFDM systems. The effect of the distortion can be modeled as attenuation of the signal and generation of a nonlinear additive noise[3]. This nonlinear noise

Received May 15, 2007; accepted July 13, 2007
doi: 10.1007/s11432-007-0055-0
†Corresponding author (email: wangj01@mails.tsinghua.edu.cn)
Supported by the National Natural Science Foundation of China (Grant No. 60172023)

passes through the channel jointly with the useful signal and, after the receiver FFT processing, distorts the symbols transmitted over each subcarrier. Most of the conventional previous works treat the nonlinear noise as an additive Gaussian process and apply various approaches to derive the variance of such a Gaussian noise[4−7]. The approximation is not quite accurate because HPA works in linear or quasi-linear region in the realistic scenario. The noise induced by clipping has an impulsive nature and is characterized by large amplitude excursions which are assumed to occur randomly in time[8,9]. In this paper, we model the statistical characteristics of the nonlinear noise more accurately by identifying the nonlinear noise as a rare-event impulsive noise for those cases of high clipping levels. Based on the properties of the large deviations of a stationary Gaussian process and shot noise theories, a new theoretical framework for OFDM, as well as DS-CDMA systems with peak-limited nonlinearities, is presented. Using the proposed framework, the effect of transmitter-added clipping noise on system performance is studied. The computer simulation results confirm the accuracy and validity of the proposed model.

1 Model description and performance analysis

1.1 System model

A typical OFDM system is shown in Figure 1. N statistically independent complex frequency domain symbols $\{x_k\}_{k=0}^{N-1}$ with total power $2\sigma^2 N$ are selected from the set of an M-QAM alphabet. The N symbols data set $\{x_k\}_{k=0}^{N-1}$ passes through the OFDM IFFT modulator whose outputs, after parallel to serial conversion, represent the N Nyquist rate time-domain complex samples of the baseband OFDM waveform. These samples are represented as

$$s_n^I + \mathrm{j}s_n^Q = \frac{1}{\sqrt{N}} \sum_{k=0}^{N-1} x_k \mathrm{e}^{\mathrm{j}\frac{2\pi kn}{N}}, \quad 0 \leqslant n \leqslant N-1. \tag{1}$$

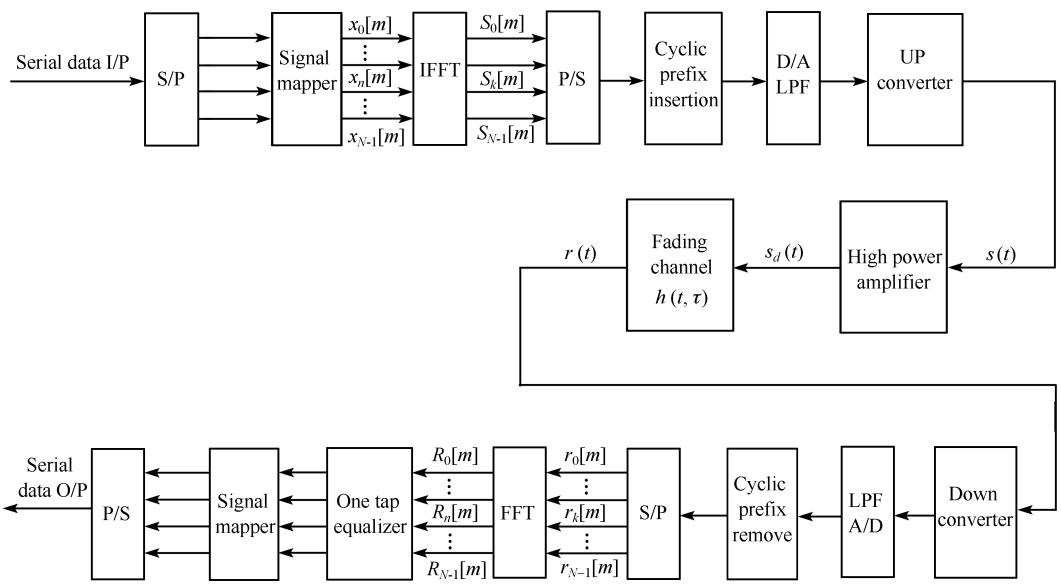

Figure 1 OFDM system architecture.

As mentioned before, s_n^I and s_n^Q can be treated as a Gaussian process independently of the subcarriers number and of the alphabet size for a sufficiently large number of subcarriers. In this situation, the probability density function (pdf) of s_n^I and s_n^Q can be described as

$$f_s(x) = \frac{1}{\sqrt{2\pi\sigma^2}} \exp\left(-\frac{x^2}{2\sigma^2} \right). \tag{2}$$

For a band-limited OFDM signal $s(t)$, HPA can be modeled as a nonlinear memoryless channel in which nonlinear distortion occurs. The extension of the Bussgang theorem to complex Gaussian process[10,11] gives the separateness of a nonlinear output as the sum of a complex-scaled useful input replica and an uncorrelated nonlinear distortion component, expressed by

$$s_d(t) = s_u(t) + w(t) = Ks(t) + w(t), \tag{3}$$

where $w(t)$ is an additive noise waveform representing the clipping events and K is an attenuation factor satisfying the following equation

$$E\{s(t+\tau)s_d(t)\} = K \cdot E\{s(t+\tau)s(t)\}. \tag{4}$$

When the clipping level l is high enough, $K \approx 1$ and a soft clipping nonlinearity is a good approximation as

$$\tilde{a}_n \triangleq g(a_n) = \begin{cases} -A_{\max}, & a_n \leqslant -A_{\max}, \\ a_n, & |a_n| < A_{\max}, \\ A_{\max}, & a_n \geqslant A_{\max}, \end{cases} \tag{5}$$

where $a_n = |s_n| = \sqrt{\left(s_n^I\right)^2 + \left(s_n^Q\right)^2}$ is the amplitude of the nth sample of the complex OFDM signal and $A_{\max}$ is the maximum permissible amplitude over which the signal is clipped.

The clipping ratio γ is defined as

$$\gamma \triangleq \frac{A_{\max}}{\sqrt{P_{\text{in}}}} = \frac{l}{\sqrt{2}\sigma}, \tag{6}$$

where P_{in} is the effective mean input power of the OFDM signal before HPA. Since the amplitude a_n is a Rayleigh random variable with pdf

$$f_{a_n}(a_n) = \frac{2a_n}{P_{\text{in}}} \exp\left(-\frac{a_n^2}{P_{\text{in}}} \right). \tag{7}$$

The total output power P_{out}, which is the sum of the signal and distortion components, is given by

$$P_{\text{out}} = E_{a_n}\left\{ g^2\left(a_n\right) \right\} = \left(1 - \mathrm{e}^{-\gamma^2}\right) P_{\text{in}}. \tag{8}$$

For high level crossings, the relationship between clipping ration and OBO (Output Back-Off) is given by

$$OBO = A_o^2 / P_{\text{out}} \approx l^2 / P_{\text{in}} = \gamma^2. \tag{9}$$

1.2 The large deviations of a stationary Gaussian process and shot noise theories

Asymptotic statistical properties of the threshold crossing behavior of a Gaussian process can be used to model $w(t)$ in the case when HPA clipping level is very high. The clipping events can be represented by a Poisson sequence of pulses as $w(t) = \sum_{k=-\infty}^{\infty} p_k(t - t_k)$, where t_k is the moment

when the kth event occurs[8,9]. For OFDM systems with large number of subcarriers, the power spectrum of $s(t)$ can be approximated as a rectangle with bandwidth $B=N/T$, where T is the duration of an OFDM symbol. The average rate of the Poisson process is given by[8]

$$\lambda = \frac{1}{2\pi}\sqrt{\frac{\dot{\sigma}^2}{\sigma^2}}\mathrm{e}^{-\frac{l^2}{2\sigma^2}} = \frac{B}{\sqrt{3}}\mathrm{e}^{-\frac{\gamma^2}{2}}, \tag{10}$$

where $2\dot{\sigma}^2$ is the variance of the derivative process of $s(t)$.

For two-side clipping, the number of clips in an OFDM symbol can be written as

$$\nu = 2\lambda T = \frac{2N}{\sqrt{3}}\mathrm{e}^{-\frac{\gamma^2}{2}}. \tag{11}$$

The probability density $f_\tau(\tau)$ of the duration τ for each clipping event (i.e., the time interval between an upcrossing and subsequent downcrossing of the HPA clipping level) follows an asymptotic Rayleigh distribution, and the shape of each pulse is approximated by a parabolic arc[8,9]. Using the relationship between τ and s, we can derive the distribution of the area s of the parabolic pulse as

$$f_s(s) = \frac{f_\tau(s)}{|s'_\tau|} = \left|\frac{1}{3s}\sqrt[3]{\frac{12s\sigma^2}{l\dot{\sigma}^2}}\right| f_\tau\left(\sqrt[3]{\frac{12s\sigma^2}{l\dot{\sigma}^2}}\right). \tag{12}$$

For the frequency band of interest and high level l crossing, the average duration τ for each clipping event is much smaller than symbol duration T. The clipping pulse train can be approximated by

$$w(t) = \sum_{k=-\infty}^{\infty} s_k \cdot \delta(t - t_k), \tag{13}$$

where $\delta(\cdot)$ is the impulse function, t_k are Poisson distributed event times, and s_k are random variables representing parabola area with distribution $f_s(s)$.

1.3 Received impulse noise model

At the front end of the receiver, received nonlinear noise waveforms are the convolution results of the Poisson impulse train and channel impulse response. For an M-QAM-OFDM system, the impulse responses of correlators are given by[12]

$$h_1(t) = \begin{cases} \sqrt{2/T}\cos(2\pi t/T), & 0 \leqslant t \leqslant T, \\ 0, \quad \text{other}, \end{cases} \qquad h_2(t) = \begin{cases} \sqrt{2/T}\sin(2\pi t/T), & 0 \leqslant t \leqslant T, \\ 0, \quad \text{other}, \end{cases} \tag{14}$$

and the received waveform can be expressed as

$$n'_I(t) = \sum_{k=-\infty}^{\infty} s_k \cdot h_1(t - t_k) + \sum_{l=-\infty}^{\infty} s_l \cdot h_2(t - t_l). \tag{15}$$

The variance of the impulse noise is then given by

$$\sigma_I^2 = \lambda\int_0^T\int_0^\infty n_I'^2(t) f_s(s) ds dt = 2\lambda\int_0^\infty s^2 f_s(s) ds \triangleq 2\lambda\left\langle s^2\right\rangle, \tag{16}$$

where the symbol $\langle\cdot\rangle$ denotes the expectation.

An integral probability density expression for the amplitude distribution has been derived by Rice[13] which is given by

$$\Phi_{n_I'}(\omega_1,\omega_2)=\exp\left\{2\lambda\int_0^{\infty}f_s(s)ds\int_0^{T}\left\{\exp\left[\mathrm{j}s\left(\omega_1 h_1(t)+\omega_2 h_2(t)\right)\right]-1\right\}dt\right\}. \tag{17}$$

Let $\omega_1=\rho\cos\varphi$, $\omega_2=\rho\sin\varphi$, and $\rho^2=\omega_1^2+\omega_2^2$, eq. (17) can be written as

$$\Phi_{n_I'}(\rho,\varphi)=\exp\left\{2\lambda T\int_0^{\infty}f_s(s)\left[J_0\left(s\rho\sqrt{\frac{2}{T}}\right)-1\right]ds\right\}, \tag{18}$$

where $J_0(z)=\frac{1}{\pi}\int_0^{\pi}\exp(jz\cos\theta)d\theta$ is the first kind of Bessel function of zero order.

We expand the J_0 term in (18) in power series as

$$J_0\left(s\rho\sqrt{2/T}\right)=\sum_{k=0}^{\infty}\frac{(-1)^k\rho^{2k}s^{2k}}{2^kT^k\left(k!\right)^2}=1-\frac{\rho^2s^2}{2T}+\sum_{k=2}^{\infty}\frac{(-1)^k\rho^{2k}s^{2k}}{2^kT^k\left(k!\right)^2}, \tag{19}$$

Since $\mathrm{e}^{-\frac{\left\langle s^2\right\rangle\rho^2}{2T}}=\sum_{k=0}^{\infty}\frac{(-1)^k\rho^{2k}\left\langle s^2\right\rangle^k}{2^kT^k\left(k!\right)}=1-\frac{\rho^2\left\langle s^2\right\rangle}{2T}+\sum_{k=2}^{\infty}\frac{(-1)^k\rho^{2k}\left\langle s^2\right\rangle^k}{2^kT^k\left(k!\right)}$, we can obtain the following equation as

$$\left\langle J_0\left(s\rho\sqrt{2/T}\right)\right\rangle=\int_0^{\infty}f_s(s)J_0\left(s\rho\sqrt{2/T}\right)ds=\mathrm{e}^{-\frac{\left\langle s^2\right\rangle\rho^2}{2T}}\left[1+\frac{C_4}{4^3}\rho^4-\frac{C_6}{4^3\left(3!\right)^2}\rho^6+o\left(\rho^8\right)\right], \tag{20}$$

where $C_4=72\left\langle s^2\right\rangle^2\Big/T^2$, $C_6=7\cdot12^3\left\langle s^2\right\rangle^3\Big/T^3$. The terms with orders higher than C_4 and C_6 terms produce only negligible results. Combining (11) and (16), eq. (18) can be further approximated as

$$\Phi_{n_I'}(\rho)\approx\exp\left\{-2\lambda T+2\lambda T\exp\left[-\frac{\left\langle s^2\right\rangle\rho^2}{2T}\right]\right\}=\exp\left\{-\nu+\nu\exp\left[-\frac{\sigma_I^2\rho^2}{2\nu}\right]\right\}. \tag{21}$$

Rewriting (21) as

$$\Phi_{n_I'}(\omega_1,\omega_2)=\exp\left\{-\nu+\nu\exp\left[-\frac{\sigma_I^2(\omega_1^2+\omega_2^2)}{2\nu}\right]\right\}. \tag{22}$$

To detect the symbols of each subcarrier, the clipped and noisy received signal passes through the OFDM FFT demodulator. The characteristic function (CF) of impulse noise at the output of the demodulator is expressed as

$$\Phi_{n_I}(\omega_1,\omega_2)=\left[\Phi_{n_I'}\left(\frac{\omega_1}{\sqrt{N}},\frac{\omega_2}{\sqrt{N}}\right)\right]^N=\exp\left[-N\nu+N\nu\exp\left(-\frac{\sigma_I^2(\omega_1^2+\omega_2^2)}{2N\nu}\right)\right]. \tag{23}$$

1.4 System performance analysis

Using (23), we derive statistical properties of total noise at the output of the demodulator as

$$\begin{aligned}\Phi_n(\omega_1,\omega_2)&=\Phi_{n_I}(\omega_1,\omega_2)\cdot\Phi_{n_G}(\omega_1,\omega_2)\\&=\mathrm{e}^{-N\nu}\sum_{k=0}^{\infty}\frac{(N\nu)^k}{k!}\exp\left[-\frac{1}{2}\left(\sigma_G^2+\frac{k}{N\nu}\sigma_I^2\right)(\omega_1^2+\omega_2^2)\right],\end{aligned} \tag{24}$$

where $\Phi_{n_G}(\omega_1, \omega_2)$ is the CF of AWGN. Then, pdf of the noise $f_n(x, y)$ can be written as

$$f_n(x,y) = \mathrm{e}^{-N\nu} \sum_{k=0}^{\infty} \frac{(N\nu)^k}{k!} \cdot \frac{1}{2\pi\sigma_k^2} \exp\left[-\frac{\left(x^2 + y^2\right)}{2\sigma_k^2} \right], \tag{25}$$

where $\sigma_k^2 \triangleq \sigma_G^2 + \frac{k}{N\nu}\sigma_I^2$, and x and y are the real and imaginary parts of the complex noise.

For the general case of QAM with $M=2^k$, where k is even, the average symbol error rate (SER) for the M-QAM-OFDM system in AWGN and Rayleigh fading channels is given by[12,14]

$$P_{\mathrm{SER}}(E) = 1 - \frac{1}{2^{M-2}} \left[P_a + \left(2^{(k-1)} - 1\right)^2 P_b + 2\left(2^{(k-1)} - 1\right) P_c \right], \tag{26}$$

$$\overline{P}_{\mathrm{SER}}(E) = \int_0^{+\infty} P_{\mathrm{SER}}(E) f_X(\chi) d\chi, \quad f_X(\chi) = \frac{1}{\overline{\chi}} \mathrm{e}^{-\chi/\overline{\chi}}, \ \chi \geqslant 0, \tag{27}$$

with $P_a = \Pr\left\{ x \geqslant -\frac{d}{2}, \ y \geqslant -\frac{d}{2} \right\}$, $P_b = \Pr\left\{ |x| \leqslant \frac{d}{2}, \ |y| \leqslant \frac{d}{2} \right\}$, $P_c = \Pr\left\{ x \geqslant -\frac{d}{2}, \ |y| \leqslant \frac{d}{2} \right\}$,

where d represents the minimum distance between the two adjacent constellation points, χ is instantaneous, SNR and $\overline{\chi}$ the average SNR of the channel.

2 Numerical examples and discussion

The SER of an OFDM system in the AWGN channel derived by the proposed approach is shown in Figure 2 for the different M-QAM constellation sizes. Referring to IEEE standard 802.11a[15], 64/16-QAM modulation, 64 subcarriers with 52 data subcarriers, and a 64-point FFT are simulated. In order to observe the effects of clipping alone, cyclic prefix, training data insertion, perfect channel estimation, and synchronization are assumed. Figure 2 illustrates analytical and simulation results, as compared to the result with SEL model in Figure 6 of ref. [4], which is obtained by "additive Gaussian noise" model.

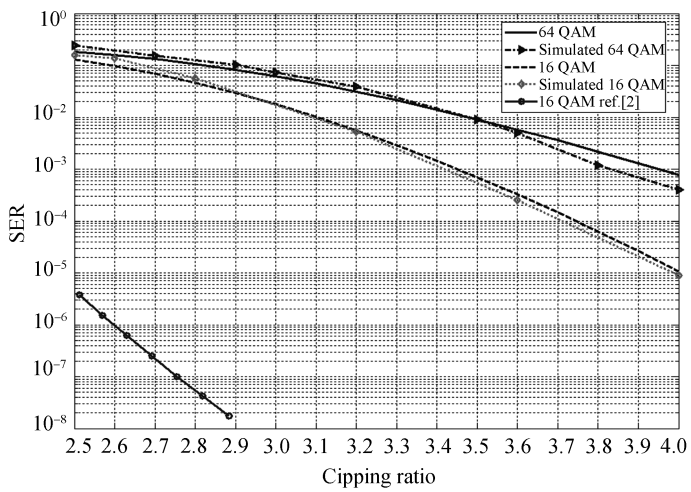

Figure 2 Simulated and analytical SER floor due to clipping; comparison with result with SEL model in Figure 6 of ref. [2].

It is easy to see from Figure 2 that SER obtained using additive Gaussian noise is substantially lower than our approach when clipping ratio becomes large. As is commented in ref. [5], additive Gaussian model is valid only if the working point of HPA is near saturation and the number of the distortion errors that occurs in the time-domain during the duration of each OFDM symbol is high enough. Since peak power is needed only in the worst-case links, the "backoff" is typically designed in the range of 10—20 dB[16]. Therefore, HPA works in linear or quasi-linear region in most realistic scenarios. There are typically not so many clipping events within an OFDM symbol that could justify a Gaussian *i.i.d*. assumption for the DFT domain. This kind of analysis is only valid for very low clipping levels with many clips. This does not usually occur in real cases. Ignoring this, the bit-error rate computations would lead to the completely wrong interpretation that clipping noise is not an issue at all for very low error rates obtained. The effect is underestimated as can be seen from Figure 3 taken from ref. [7]. In fact, when clipping level is high enough and a clip is a rare event, clipping induced noise is concentrated in time as impulses. Using additive Gaussian noise model will spread the impulses uniformly over the time, which can substantially underestimate the error probability.

Simulated and analytical results in Rayleigh fading channels are given in Figure 4. A two-path WSSUS multi-path channel with an exponentially decaying profile is assumed during simulation.

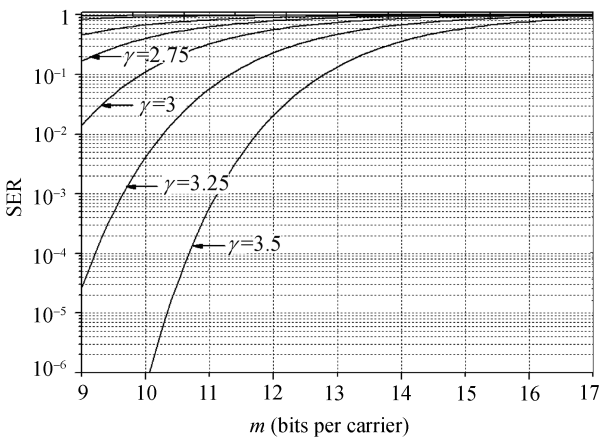

Figure 3 SER as a function of the number of bits per carrier and clipping ratio with Gaussian noise model[7].

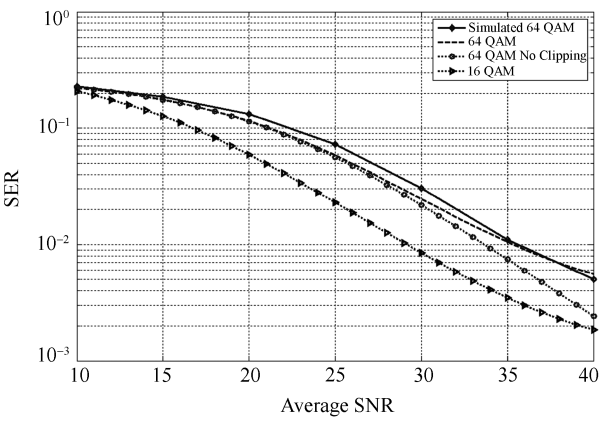

Figure 4 Comparison of simulated and analytical SER in Rayleigh fading channel, γ=4.

For a given clipping ratio, each received error bit is the function of the received SNR. The good agreement between simulated and theoretical results verifies the impulsive nature of clipping induced noise and demonstrates the effectiveness of the model.

3 Application for large capacity DS-CDMA systems

In large capacity DS-CDMA systems, downlink signals share many common properties with OFDM signals, e.g., they are composite signals where each component is characterized by an orthogonal or quasi-orthogonal sequence of chips[17], which can be quite accurately represented as a complex Gaussian process with a power spectral density approaching to a rectangular form over the bandwidth $B=1/T_c$, as well as high PAPR, where T_c is the duration of one chip.

Obviously, the technique described above can accurately illustrate nonlinear distortion of downlink signals of DS-CDMA systems with peak-limited nonlinearities. However, the main difference between DS-CDMA and OFDM systems is that multiple access interference (MAI) in DS-CDMA systems must be included when considering the bit decision statistic at the receiver. In a BPSK spread DS-CDMA system, the MAI component can be accurately modeled as a Gaussian RV with mean zero and variance of $(K-1)/3N$[18], where K is the number of users and N is spread factor of the system.

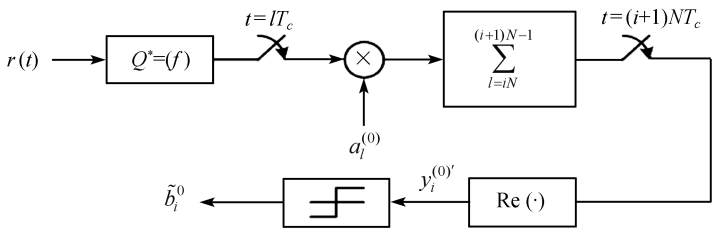

Figure 5 The coherent correlator receiver for user 0[17].

The CF of impulse noise $n_I(t)$ in the CDMA system can be expressed after accumulation and bit decision as[19]

$$\Phi_{n_I}(v)=\sum_{m=0}^{N}\binom{N}{m}p^m(1-p)^{N-m}\exp\left(-\frac{mv^2\sigma_{BG}^2}{2N^2}\right). \tag{28}$$

The system error probability P_e then is given by[19]

$$P_e=\sum_{m=0}^{N}\binom{N}{m}p^m(1-p)^{N-m}Q\left(\sqrt{\chi_m^{-1}}\right), \tag{29}$$

where $\chi_m^{-1}=m\sigma_{BG}^2/N^2E_b+N_0/2E_b+(K-1)/3N$ is the reciprocal of the SNR at the receiver.

Figure 6 is the comparison of the simulations of 16 users and 25 users with theoretical results of a DS-CDMA system with BPSK spreading and no AWGN ($E_b/N_0\to\infty$) is assumed. The system spread factor N=32. The simulated P_e is obtained by Monte-Carlo experiment and is made with 10000 runs for each γ. The asymptotic curves in the plot are given by $Q\left(\sqrt{3N/(K-1)}\right)$. The figure shows that the impact of the noise becomes minor compared with MAI when the working point of HPA is far away from saturation.

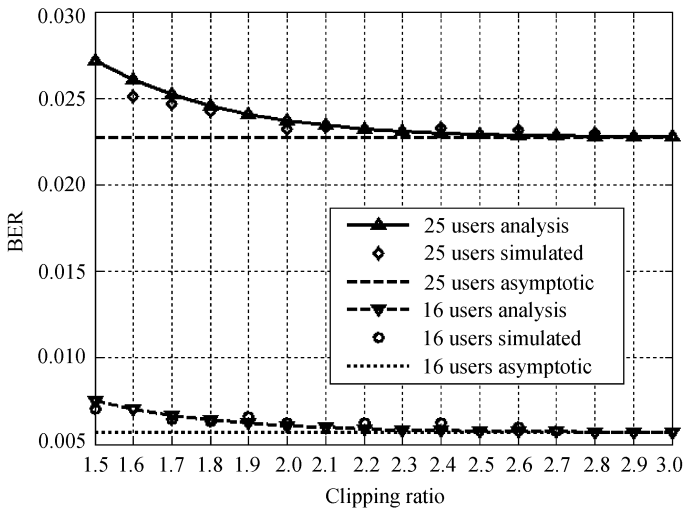

Figure 6 P_e versus γ for 16 and 25 users, $E_b/N_0 \to \infty$.

Figure 7 shows the contribution of AWGN, MAI, and impulse noise to the system performance in AWGN channels. When the working point of the CDMA system is near saturation region with small clipping ratio, the system performance degrades dramatically for the impact of the impulse noise; and AWGN becomes dominant compared with impulse noise when the system working point is far away from the saturation region.

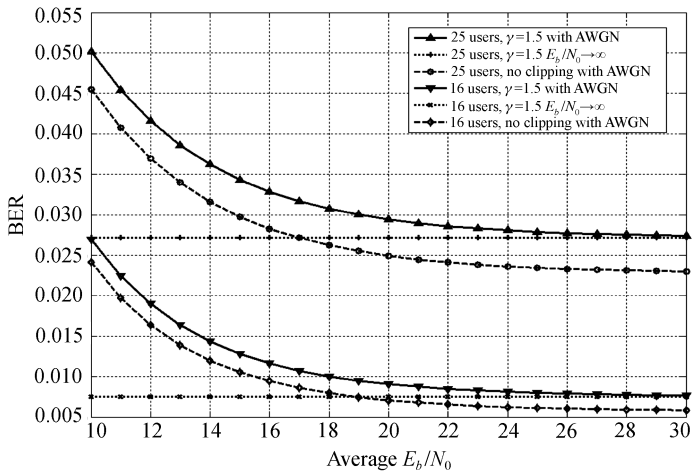

Figure 7 P_e versus E_b/N_0 for 16 and 25 users, γ=1.5.

4 Conclusions

A new theoretical framework on performance analysis of OFDM and CDMA systems in AWGN and fading channels with nonlinear effects is presented. By applying the statistical properties of asymptotic clipping to shot noise theories, the approach offers important insights into the true nature of the system clipping process especially at high backoffs where the Gaussian approximation of the nonlinear noise is no longer valid. Computer simulations verify accuracy of the model and effectiveness of the approach. The theoretical framework developed in this paper can be used

to evaluate many communications systems with peak-limited nonlinearities and high PAPR.

1 Papoulis A. Probability, Random Variables and Stochastic Process. New York: McGraw-Hill, 2002
2 Armstrong J. New OFDM peak-to-average power reduction scheme. In: Proc. IEEE VTC'01, Rhodes, Greece, May 2001
3 Santella G, Mazzenga F. A hybrid analytical-simulation procedure for performance evaluation in *M*-QAM-OFDM schemes in presence of nonlinear distortions. IEEE Trans Veh Technol, 1998, 47: 142－151
4 Dardari D, Tralli V, Vaccari A. A theoretical characterization of nonlinear distortion effects in OFDM systems. IEEE Trans Commun, 2000, 48: 1755－764
5 Banelli P, Cacopardi S. Theoretical analysis and performance of OFDM signals in nonlinear AWGN channels. IEEE Trans Commun, 2000, 48: 430－441
6 Bos C, Ksuwenhoven M H L, Serdijn W A. Effect of smooth nonlinear distortion on OFDM symbol error rate. IEEE Trans Commun, 2001, 49: 1510－1514
7 Henkel W, Wagner B. Another application for trellis shaping: PAR reduction for DMT (OFDM). IEEE Trans Commun, 2000, 48(9): 1471－1476
8 Rice S O. Distribution of the duration of the duration of fades in radio transmission. Bell Syst Tech J, 1958, 37: 581－635
9 Kac M, Slepian D. Large excursions of Gaussian processes. Ann Math Stat, 1959, 30: 1215－1228
10 Bussgang J J. Crosscorrelation functions of amplitude distorted Gaussian signals. Res Lab of Electronics, MIT, Mass Tech Rep, Mar. 1952
11 Rowe H E. Memoryless nonlinear with Gaussian inputs: Elementary results. Bell Syst Tech J, 1982, 61(7): 1519－1525
12 Proakis J G. Digital Communications. New York: McGraw-Hill, 2001
13 Rice S O. Mathematics analysis of random noise. Bell Syst Tech J, 1944, 23: 282—332
14 Ghosh M. Analysis of the effect of impulse noise on multicarrier and single carrier QAM systems. IEEE Trans Commun, 1996, 44(2): 145－147
15 IEEE std 802.11-1999, Part 11: Wireless LAN Medium Access Control (MAC) and Physical Layer (PHY) Specifications, 1999
16 Raab F H, Asbeck P, Cripps S, et al. Power amplifiers and transmitters for RF and microwave. IEEE Trans Microwave Theory Tech, 2002, 50(3): 814－826
17 Conti A, Dardari D, Tralli V. An analytical framework for CDMA systems with a nonlinear amplifier and AWGN. IEEE Trans Commun, 2002, 50(7): 1110－1120
18 Yoon Y C. A simple and accurate method for probability of bit error analysis for asynchronous band-limited DS-CDMA systems. IEEE Trans Commun, 2002, 50(4): 656－663
19 Wang J, Shan X M, Ren Y. A new approach for evaluating clipping distortion in DS-CDMA systems. IEICE Trans Commun, 2005, E88-B(2): 792－796